Revista Brasileira de Geografia Física

ISSN:1984-2295

Homepage:https://periodicos.ufpe.br/revistas/rbgfe

Vegetation response to extreme rainfall and drought events in deforested areas of the Doce River Basin

Nelson Pedro António Mateus[1], Ana Paula M A Cunha[2], Ursula Runchkys[3], Anacleto Diogo[4], Ricardo Amorim[5].

[1,3,4] Programa de pós-graduação em análise e modelagem de sistemas ambientais, Universidade Federal de Minas Gerais, Av. Pres. Antônio Carlos, 6627 - Pampulha, Belo Horizonte - MG, 31270-901. [2] Programa de pós-graduação em desastres naturais, Universidade Estadual de São Paulo, ICT Instituto de Ciência e Tecnologia Av. Eng. Francisco José Longo, 777 São Dimas. CEP 12245-000. [4] Programa de pós-graduação em meteorologia, Universidade Federal de Alagoas. Av. Paulo Holanda, 19 - Cidade Universitária, Maceió – AL. [5]Southern African Science Service Centre for Climate Change and Adaptive Land Management (SASSCAL). Faculty of Agricultural Sciences (FCA), José Eduardo dos Santos University (UJES), Largo Deolinda Rodrigues,Cidade Alta, Huambo-Angola. Autor correspondente E-mail: nelson.pa.mateus@gmail.com[1], vineana2015@gmail.com [2], tularuchkys@yahoo.com.br [3], anacletomarito@gmail.com [4], rfcamorim@gmail.com [5].

Article received on 15/02/2025 and accepted on 16/07/2025

A B S T R A C T

Climate change has increased the frequency and intensity of extreme events, affecting ecosystems globally. In the Doce River Basin (DRB), historically impacted by deforestation and the 2015 Mariana disaster, the interaction between drought, extreme rainfall, and vegetation response remains insufficiently understood. This study applies wavelet coherence analysis, for the first time in this context, to examine relationships between extreme climate events and vegetation dynamics. Time series of the Enhanced Vegetation Index (EVI) and climate indices (SPI 1, 3, and 6 months; RX1day; RX5day; PRCPTOT; CDD) from 2000 to 2023 were analyzed to identify spatial and temporal trends across the basin. The results reveal that vegetation responds to extreme precipitation events (RX1day, RX5day, PRCPTOT, and CDD) mainly over 8- to 16-month timescales, reflecting seasonal recovery patterns. Conversely, responses to drought events (SPI_1, SPI_3, SPI_6) occur more rapidly, within 2 to 4 months and up to 8 months, with greater sensitivity observed after the disaster. This asymmetry suggests that, under climate change, degradation impacts (drought-induced stress) occur more rapidly than vegetation recovery, indicating delayed regeneration. These changes are most notable in the northwestern, southwestern, southern, and northern DRB, where significant forest loss and agricultural expansion have occurred. In these regions, SPI_3 and SPI_6 show negative trends, indicating increased drought frequency, while RX1day and RX5day display high spatial variability related to remaining forest cover.
Keywords: Extreme events, drought, vegetation, deforestation, River Doce Basin.

Resposta da vegetação a eventos extremos de chuva e seca em áreas desmatadas da Bacia do Rio Doce.

R E S U M O

As mudanças climáticas aumentaram a frequência e intensidade de eventos extremos, afetando ecossistemas globalmente. Na Bacia do Rio Doce (BRD), historicamente impactada pelo desmatamento e pelo desastre de Mariana (2015), a interação entre secas, chuvas extremas e a resposta da vegetação ainda é pouco compreendida. Este estudo aplica, pela primeira vez neste contexto, a análise de coerência wavelet para investigar as relações entre eventos climáticos extremos e a resposta da vegetação. Foram analisadas séries temporais do Índice de Vegetação Aprimorado (EVI) e de índices climáticos (SPI de 1, 3 e 6 meses; RX1day; RX5day; PRCPTOT; CDD), de 2000 a 2023, para identificar tendências espaciais e temporais na bacia. Os resultados mostram que a vegetação responde a eventos extremos de precipitação (RX1day, RX5day, PRCPTOT, CDD) principalmente em escalas de 8 a 16 meses, refletindo padrões sazonais. Em contraste, as respostas a secas (SPI_1, SPI_3, SPI_6) são mais rápidas, ocorrendo em 2 a 4 meses e, no máximo, até 8 meses, com maior atraso após o desastre. Essa assimetria indica que, sob mudanças climáticas, impactos da degradação (estresse hídrico) ocorrem mais rapidamente do que a recuperação da vegetação, indicando regeneração retardada. Essas mudanças são mais marcantes nas regiões noroeste, sudoeste, sul e norte da BRD, onde SPI_3 e SPI_6 apresentam tendências negativas e RX1day e RX5day mostram alta variabilidade espacial associada à cobertura florestal remanescente.

Palavras-chave: Eventos extremos, seca, vegetação, desmatamento, Bacia do Rio Doce.

Introduction

The collapse of the Fundão dam represented an unprecedented environmental impact event in the Doce River Basin (DRB), causing profound physico-chemical changes in the water bodies and a drastic reduction in riparian vegetation, which dropped from 61% to just 6% coverage (Cordeiro et al., 2022; A. T. Lima et al., 2021; Macêdo et al., 2024; Neves et al., 2024; Santana et al., 2021). However, to understand the resilience and recovery of vegetation in the DRB, it is essential to recognize that the dynamics of this cover are not shaped exclusively by disasters; climatic variables such as temperature and precipitation also exert a strong influence, with anomalies triggering extreme events(Mateus et al., 2025).

The DRB is highly vulnerable to shifts in precipitation and temperature. In recent years, its western sector has already seen a significant 6.3% loss of native vegetation. Climate projections for 2020-2050 paint a stark picture: over 300 mm less annual rainfall and an increase of up to 2°C(Campos et al., 2024). Despite these clear environmental pressures, the interplay between extreme climate events and vegetation response, especially before and after the dam collapse, remains largely under-explored in the DRB. This gap underscores the urgent need for integrated studies that can comprehensively address both climatic extremes and human pressures on local vegetation resilience and recovery.

Climate change has intensified the frequency and intensity of extreme events, which in turn has altered vegetation dynamics in various regions of Brazil (Díaz Baca et al., 2024; Dutra et al., 2024; Lins et al., 2024; Paiva et al., 2024). Global temperatures have risen sharply in recent decades, with the last four decades being the warmest since 1850 and 2024 marking the first-year global averages exceeded 1.5°C above pre-industrial levels. This warming, along with record atmospheric water vapor, has led to more severe storms, prolonged droughts, and increased wildfire risk, resulting in significant vegetation losses (IPCC, 2022, 2023; COPERNICUS, 2024).

Studies have shown that precipitation variability strongly influences vegetation cover, as revealed by time series of vegetation indices such as NDVI, RENDVI, and EVI. These indices typically peak in the summer, when warmer temperatures and higher rainfall favor plant growth, highlighting the strong correlation between climatic factors and vegetation dynamics (Junior et al., 2024; Marion et al., 2024; Morais et al., 2025; Paula et al., 2025; Santos et al., 2024; Silva et al., 2024).

The rising frequency of extreme rainfall and higher temperatures is significantly altering the distribution and composition of vegetation in the basin. These changes highlight the urgent need to better understand vegetation responses in order to develop effective adaptation and mitigation strategies(Belhaj et al., 2025; Díaz Baca et al., 2024; Gao et al., 2022; Guo et al., 2025; He et al., 2025). However, uncertainties remain, particularly at finer temporal and spatial scales, highlighting the need for further research to better understand local impacts of extreme events (Mateus et al., 2025).

Vegetation cover naturally regulates the water cycle by enhancing infiltration and reducing runoff, which helps decrease flood risk. Climate change, both globally and regionally, has a significant impact on vegetation (de Souza et al., 2024; Ferreira, 2024; Ribeiro et al., 2024). In the context of the DRB, Almeida et al. (2020) used multicriteria analysis with RapidEye satellite imagery and found that about 24% of the basin—60% of the area analyzed, requires vegetation restoration with medium to very high priority. A recent study using time series of vegetation indices found that the Fundão dam collapse in Mariana, Minas Gerais, led to the degradation of over 300 hectares.(Carmo et al., 2017; Neves et al., 2024).

The DRB is intrinsically sensitive to climatic extremes, exhibiting an irregular distribution of rainfall; its western portion, for example, is more susceptible to extreme events due to higher precipitation accumulation compared to the eastern part (Cupolillo et al., 2008; Lima & Assis, 2025; Marciano et al., 2024; Mateus et al., 2025; K. S. S. Oliveira & Quaresma, 2017).

Despite the forest restoration efforts by Fundação Renova in areas affected by tailings (May et al., 2020), A critical gap remains in understanding how vegetation in the DRB responds to extreme climatic events, especially at broader spatial and temporal scales and in highly deforested areas, as most previous studies have analyzed climate and vegetation trends separately (Almeida et al., 2020; Campos et al., 2024; Cupolillo et al., 2008; Junior et al., 2024; Neves et al., 2024; Neves et al., 2024), This study adopts an integrated approach to assess the response of vegetation to extreme climatic events in the DRB.

The relationship between extreme climatic indices (e.g., SPI, RX1day, RX5day, PRCPTOT, CDD) and vegetation response in deforested areas of the DRB remains poorly understood, especially regarding temporal dynamics and potential lag effects. No previous studies have applied wavelet coherence analysis in this context, limiting our understanding of how climatic extremes and vegetation interact at different timescales, particularly after major disturbances such as the Mariana disaster (2015). This study addresses these gaps by (a) identifying spatial and temporal trends in EVI and extreme events, (b) assessing the cumulative impacts of climatic extremes in highly deforested regions, and (c) applying wavelet coherence analysis to clarify the links between extreme climate events and vegetation resilience in the DRB.

This study focuses on the DRB, with limited expansion into neighboring regions to contextualize external pressures without detailed discussion of their internal dynamics. The DRB, located in southeastern Brazil (Figure 1), covers 86,715 km², mainly in Minas Gerais, and includes 230 municipalities with about 3.2 million inhabitants. The region's diverse economy relies on mining, agriculture, pig farming, and the food industry, and water use reflects this diversity: 38.2% for multiple uses, 30.1% for public supply, 19.3% for industry, 3.3% for mining, and 1.6% for other purposes (Neves et al., 2024; PIRH, 2010; Rickard & Ludwig, 2024; Svenning & Sandel, 2013).

Materials and methods

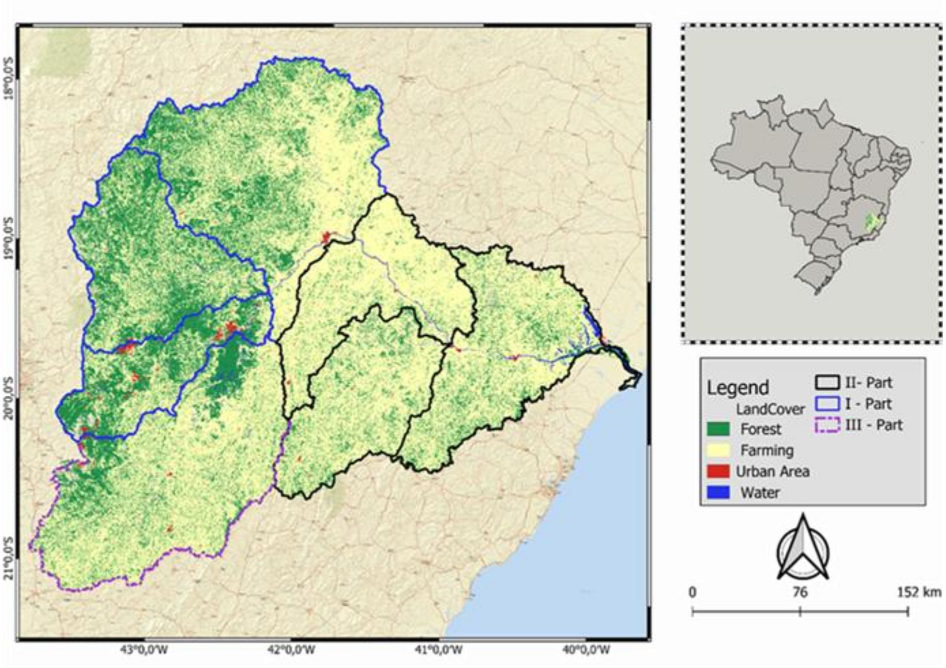

Figure 1. Study area Doce River Basin. The figure on the right represents the location of the DRB within Brazilian territory.

Methods

The extreme climatic indices used in this study (Table 1) were developed by the ETCCDI and are based on temperature and precipitation data. Indices were calculated with the Python library icclim, following ETCCDI standards to ensure methodological consistency and comparability (Chervenkov & Slavov, 2021, 2021). The methods applied followed these main steps:

a) Calculate Extreme climate indices: The indices were generated using daily CHIRPS precipitation data and a custom algorithm based on the icclim library, adapted to the study region for greater methodological accuracy. Indices were calculated monthly and annually from 2000 to 2023, allowing analysis of both seasonal variability and long-term trends. Consult the supplementary material to access the data link (https://github.com/NelsonMateus/SM_3/blob/main/Suplementary_material.pdf).

Table 1 - Summary of climate indices analyzed in this study.

Index	Total annual precipitation (mm)
PRCPTOT	Maximum daily precipitation (mm)

RX1day	Maximum daily precipitation (mm)
RX5day	Maximum precipitation over 5 consecutive days (mm).
CDD	Maximum precipitation over 5 consecutive days (mm)

b) SPI Calculation: The Standardized Precipitation Index (SPI) is a widely used metric for assessing drought severity and variability(McKee, 1995;McKee et al., 1993). In this study, the SPI-1, SPI-3, and SPI-6 scales were employed to analyze the spatiotemporal characteristics of droughts. These scales were selected because they effectively capture short-term vegetation responses to drought events, providing a dynamic view of the relationship between precipitation and vegetation indices such as EVI (Vicente-Serrano et al., 2013; Wang et al., 2025; Y. Zhang et al., 2025).

SPI is calculated by fitting monthly precipitation data to a gamma probability distribution, allowing the cumulative probability of each event to be determined from the distribution's parameters (see Equation 1 and 2).

$$G(X) = \int_0^x g(x) = \int_0^x \frac{x^{\alpha-1}e^{-x/B}}{B^{\alpha}T(\alpha)} \qquad (1)$$

$$SPI = \Psi^{-1}[G(x)] \qquad (2)$$

Where Ψ^{-1} SPI values are transformed using the inverse normal probability function (mean = 0, standard deviation = 1); full calculation details are provided by McKee et al. (1993). Drought events are classified when SPI is ≤ –1, as summarized in Table 2.

Table 2: Description of the SPI categories

Drought Grade	**SPI Value**
Extreme drought	SPI ≤ −2.00
Severe drought	−2 < SP I ≤ −1.5
Moderate drought	−1.5 < SPI ≤ −1
Mild drought	−1 < SPI ≤ −0.5
Normal	SPI ≥ −0.5

c) Trend Analysis: To assess trends in precipitation and drought indices, we applied the non-parametric Kendall Tau statistic and Theil-Sen slope estimator to gridded time series of SPI_1, SPI_3, SPI_6, and extreme precipitation indices (RX1day, RX5day, PRCPTOT, and CDD). Kendall Tau measures the strength and direction of monotonic trends, ranging from –1 (downward) to +1 (upward), while the Theil-Sen slope provides a robust estimate of trend magnitude by calculating the median slope between all data pairs. Statistical significance was set at α = 0.05. We focus the graphical presentation on the Mann-Kendall Tau statistic to highlight the spatial patterns and significance of trends. Theil-Sen slope results were used to support our interpretation and are available upon request. Further methodological details are available in the literature (El-Nesr et al., 2010; GILBERT, 1987; Spek & Derumigny, 2025).

d) *Coherence analysis*: The Wavelet Coherence Transform (WTC) was used to analyze multiscale relationships between extreme climatic events and vegetation (EVI) in the DRB. WTC measures the coherence between two non-stationary time series across time and frequency, providing insight into how climatic extremes and vegetation dynamics are linked.

Statistical significance was assessed with 1000 Monte Carlo simulations at a 5% level, and the cone of influence defined valid regions for interpretation. Phase angles in WTC plots show which variable leads or lags, helping identify the timing and direction of interactions between EVI and climate indices (SPI, RX1day, RX5day, PRCPTOT, CDD). Further methodological details can be found in the cited literature (Alsubih et al., 2025; Dong et al., 2020; Grinsted et al., 2004; Hu & Si, 2016; Irannezhad et al., 2020; Kirby & Swain, 2004; Mastroeni et al., 2025; Shu et al., 2025; Torrence & Compo, 1998). The following circle (Figure 2) illustrates the main phase directions, while the accompanying box summarizes their interpretation:

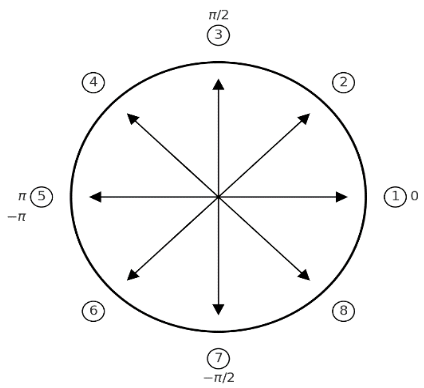

Phase	Interpretation
P1	In phase | Positive correlation
P2	In phase | Leading X(t), lagging Y(t)
P3	Transition π/2
P4	Out of phase | Leading Y(t), lagging X(t)
P5	Out of phase | Negative correlation
P6	Out of phase | Leading X(t), lagging Y(t)
P7	Transition -π/2
P8	In phase | Leading Y(t), lagging X(t)

Figure 2. Phase differences of time series X(t) against time series Y(t) in cross-wavelet analysis

Results and discussion

Rainy Season (DJF)

Analysis of CDD, PRCPTOT, RX1day, and RX5day indices indicates that the DRB is highly sensitive to precipitation extremes, especially in heavily deforested areas (Figure 3). The CDD index, in particular, showed significant positive trends ($\tau > 0.62$) during summer (DJF), indicating longer consecutive dry periods (Figure 4). This intensification of drought is especially critical in the northern DRB, where about 60% of municipalities are located in Brazil's semi-arid region and annual rainfall is often below 800 mm (Cunha et al., 2019; Mateus et al., 2025; Natividade et al., 2017; Sondermann et al., 2022).

The increase in CDD threatens surface and groundwater availability, posing risks to agriculture and urban water supply in the DRB (Natividade et al., 2017). Deforestation in key areas likely exacerbates these trends by reducing soil water retention and increasing runoff during droughts (Tian et al., 2018). Notably, the most significant increases in dry days occur in the northern and eastern DRB, where agricultural expansion and less frequent SACZ activity further aggravate water deficits (Figures 3, 4).

Significant increases in dry days are concentrated in the northern and eastern DRB during the rainy season (DJF), regions that have seen agricultural expansion and less frequent South Atlantic Convergence Zone (SACZ) activity (Mateus et al., 2025). Figure 4 shows that the most deforested areas overlap with those experiencing more consecutive dry days. The PRCPTOT index exhibited negative, though not statistically significant, trends ($\tau < -1.5$) in parts of the DRB during DJF, suggesting reduced accumulated precipitation (Figure 3). This pattern, together with increased CDD, reinforces a scenario of water deficit.

Highly deforested areas are especially vulnerable, as forest loss heightens susceptibility to microclimate changes and reduced moisture recycling, amplifying climate change impacts.(Cordeiro et al., 2022; de Souza et al., 2024; Neves et al., 2024).

The extreme precipitation indices RX1day and RX5day show similar patterns in the DRB, especially in the southern sector. RX1day exhibits a significant negative trend, indicating reduced maximum daily rainfall. This area depends on the SACZ for water supply, but studies (Mateus et al., 2025) report fewer SACZ events and intensified extremes in the south, worsening local water deficits. These changes impact water availability and aquifer recharge, increasing the vulnerability of southern DRB to water scarcity.

Moreover, the areas in the southern sector of the basin that exhibit negative trends in RX1day coincide with regions of high deforestation rates (Figures 3 and 4). The loss of forest cover intensifies the impacts of climate change by reducing moisture recycling and the soil's water retention capacity.

This creates a vicious cycle in which deforestation intensifies both drought conditions and the reduction of extreme rainfall events (Campos et al., 2024; Cupolillo, et al., 2008; Lima & Assis, 2025). The RX5day index also shows negative trends ($\tau > -1.5$) in the southern DRB, though less pronounced than RX1day, indicating that multi-day heavy rainfall events are becoming less frequent or intense, while some areas show minor, non-significant increases. As with RX1day, negative RX5day trends are concentrated in the most deforested regions (Figure 4).

Dry Season (JJA)

During winter (JJA), the DRB exhibits positive CDD trends ($0.35 < \tau < 0.62$), especially in the western sector, indicating longer dry periods (Figures 5 and 6). This pattern highlights the typical challenges of the dry season for water availability, particularly in the vulnerable northern regions near deforested and less vegetated areas, where prolonged droughts are more intense.(Almeida et al., 2020; May et al., 2020).

The PRCPTOT index shows significant negative trends ($\tau < -1.5$) in the far north of the DRB, indicating reduced accumulated precipitation and potential risks to water recharge and security for local communities (Campos et al., 2024). In contrast, central and western areas with more forest cover exhibit positive PRCPTOT trends (Figures 5 and 6), highlighting the essential role of forests in stabilizing rainfall and mitigating water deficits.

Similarly, the extreme precipitation indices RX1day and RX5day show significant negative trends in the southern and western DRB, aligning with zones of high deforestation and water stress (Mateus et al., 2025). Persistent deforestation in these regions decreases soil water retention and moisture recycling, increasing the basin's vulnerability to prolonged drought and reduced intense rainfall. Overall, these results reinforce the strong link between vegetation loss and intensified climate impacts in the DRB (Hoyos *et al.*, 2013; Ma *et al.*, 2024; Smith *et al.*, 2023; Wei *et al.*, 2024).

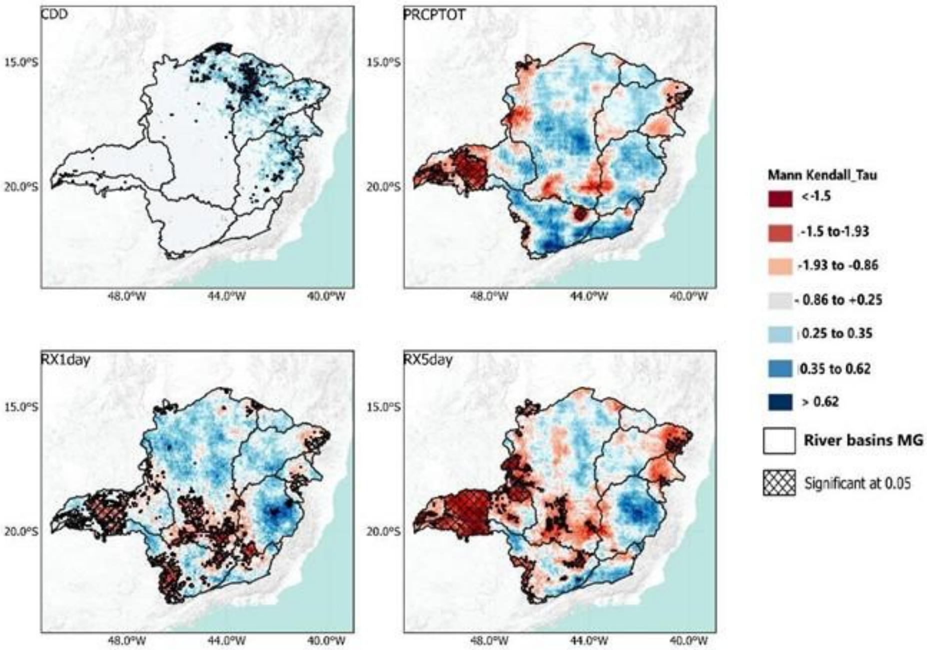

Figure 3. Spatial distribution of the Mann-Kendall tau values (DJF) for time series (2000–2023) across the river DRB include basins of Minas Gerais. The analysis includes key climate indices: CDD (Consecutive Dry Days); PRCPTOT (Total Precipitation); RX1day (Maximum 1-day).

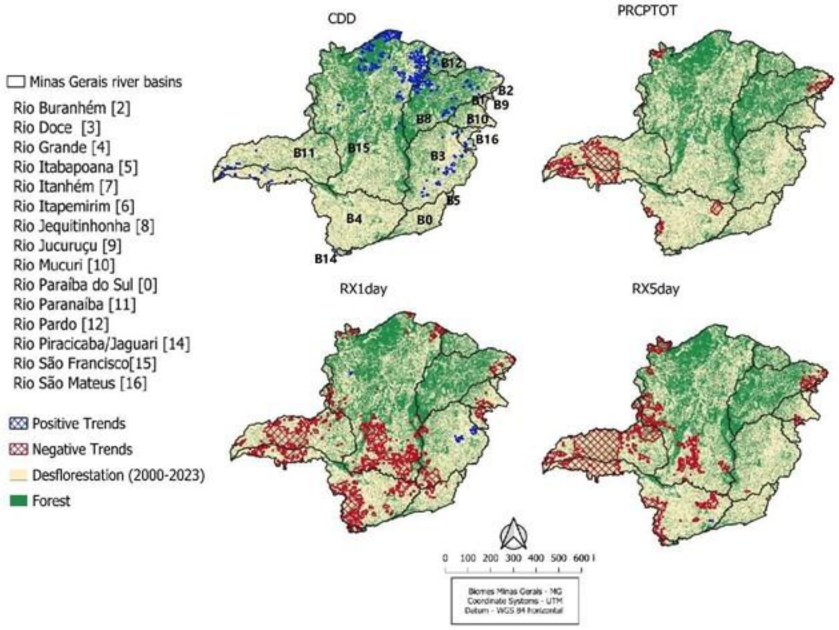

Figure 4. Deforestation map and extreme indices (same indices as in Figure 3).

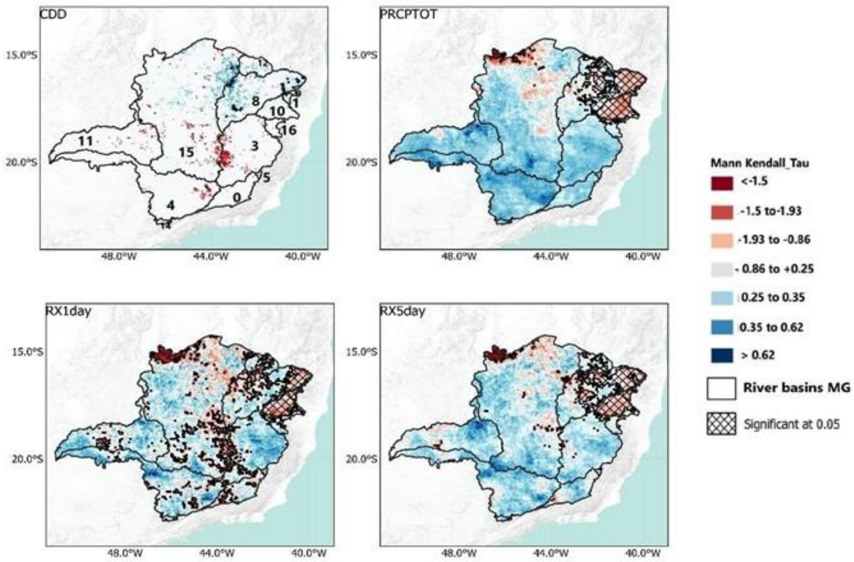

Figure 5. Same as figure 3, but for dry season (JJA).

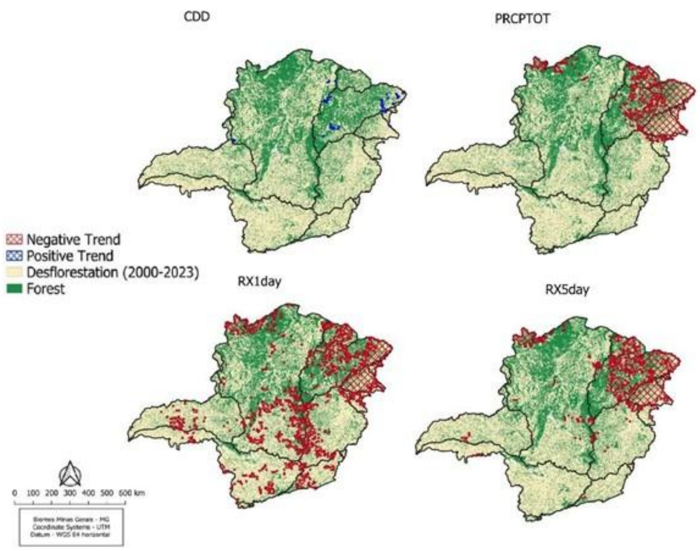

Figure 6 - Same as figure 4, but for dry season (JJA).

Connection between Extreme Events and EVI

The cross-wavelet coherence graphs provide a detailed insight into how vegetation (EVI) in the DRB responds to different climatic indices, such as CDD, PRCPTOT, RX1day, and RX5day, across various temporal scales. This analysis is crucial for understanding the complex interactions between climate extremes, hydrological cycles, and ecosystems in the DRB, a region significantly vulnerable due to environmental degradation and climate change(Campos et al., 2024; Cupolillo et al., 2008; Mateus et al., 2025).

Overall, vegetation response to extreme events showed strong coherence at the 8–16-month scales across the basin (Figure 7). The predominance of high coherence at this scale is common, as vegetation does not immediately respond to drought or rainfall events, there is a lag time before changes in vegetation can be observed. This pattern has been documented in studies analyzing vegetation response to extreme events in various regions(Kulesza & Hościło, 2024; Wang et al., 2023; Zhang et al., 2017). For the CDD index, vegetation response predominantly occurs out of phase, indicating that an increase in dry days is associated with a reduction in EVI values. In other words, vegetation shows signs of water stress. However, this response exhibits a delay, suggesting that vegetation takes time to manifest the impacts of consecutive dry periods and to recover after the end of such events in the DRB (Figure 7A).

This dynamic aligns with previous studies (Campos et al., 2024; Marengo et al., 2009), which indicate that vegetation sensitivity to drought depends on factors such as soil water retention, vegetation cover, and precipitation seasonality. In the DRB, areas affected by deforestation or conversion of native forests to pasture are especially vulnerable due to reduced water infiltration and amplified drought impacts (Cupolillo et al., 2008; Oliveira et al., 2020; Oliveira & Quaresma, 2017).

Between 2014 and 2016, wavelet coherence analysis revealed a significant relationship between EVI and CDD at the 4- to 8-month scale (Figure 7A), with both variables in phase. This suggests that vegetation dynamics closely tracked changes in drought conditions, potentially influenced by the 2015 environmental disaster in the DRB(Cunha et al., 2019).

The disaster may have increased local variability in the EVI–CDD relationship, reflecting the heterogeneity of affected areas. While some regions showed resilience and recovery, others exhibited a marked decline in EVI (de Carvalho et al., 2024; Kulesza & Hościło, 2024).

The 2014–2016 period coincided with adverse climatic conditions in Brazil, including severe droughts likely intensified by the 2015 El Niño event (Almeida et al., 2020; Guo et al., 2025; Kogan & and Guo, 2017; Marengo et al., 2015).

Strong coherence between EVI and PRCPTOT on the 8–16-month scale indicates these variables are in phase, with PRCPTOT slightly leading (Figure 7B). This pattern suggests that vegetation in the DRB depends on accumulated precipitation over longer cycles (De Almeida et al., 2020). The lead of PRCPTOT may reflect the role of rainfall in enabling vegetation recovery after water stress, particularly noticeable in 2015–2016, when post-disaster rainfall contributed to partial recovery in less affected areas, as seen in 2018–2020.

For periods longer than 32 months, the coherence between PRCPTOT and EVI falls outside the cone of influence during 2000–2007, reducing statistical reliability (Figure 7B). This suggests that at longer timescales, the relationship between precipitation and vegetation is less robust, possibly due to other influences such as local soil variation and land use changes. Between 2013 and 2016, significant coherence at the 2–4-month scale indicates extreme precipitation events (RX1day, RX5day) are out of phase with EVI, with EVI leading (Figures 7C, 7D). The 2015 Fundão dam disaster may have reduced vegetation's ability to respond, amplifying the impacts of extreme rainfall by decreasing infiltration and increasing runoff (D. de S. Neves et al., 2024).

This event marked a shift in land-use drivers: while climate previously constrained agro-pastoral expansion, post-disaster, anthropogenic factors gained prominence, with slope and urbanization influencing land use (Carmo et al., 2017; A. Lyra et al., 2018). On the 8–16-month scale, RX1day and RX5day indices lead EVI, indicating that intense rainfall events are important for vegetation recovery over longer periods, especially in less degraded areas. At scales of 32–64 months, the relationship between extreme precipitation and vegetation is not statistically robust, likely reflecting the influence of land-use change, shifts in forest cover, and large-scale climate variability

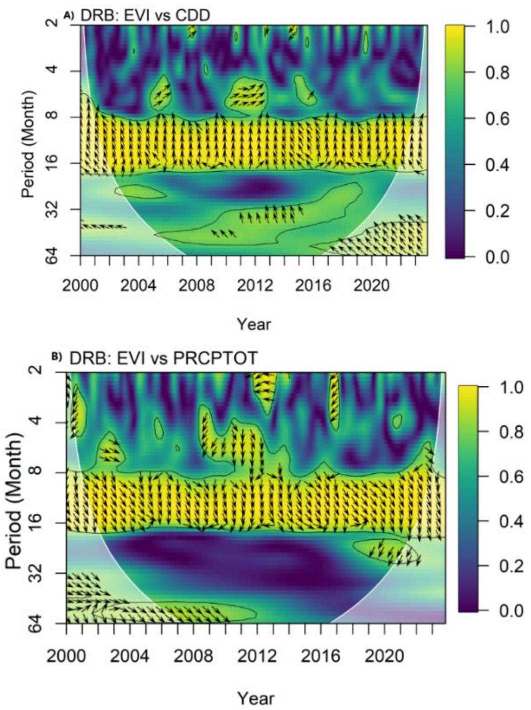

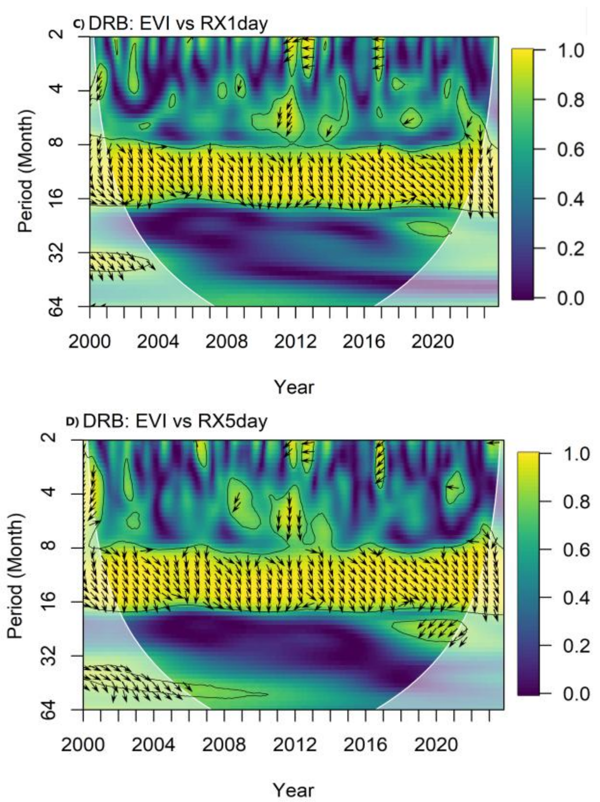

Figure 7. Wavelet Coherence Analysis between EVI and the CDD and PRCPTOT Indices for the DRB (2000-2023).

Spatial Trends (SPI) and Deforestation

Rainy Season (DJF)

Analysis of SPI trends for SPI_1, SPI_3, and SPI_6 (Figure 8) during DJF (December–February) in the DRB reveals marked variations in drought and wetness regimes, reflecting combined effects of climate change and deforestation.

Significant negative trends ($\tau < -1.5$), mostly in the southern and western DRB, indicate increased water deficits at multiple time scales. At the SPI_1 scale, these trends point to more frequent and intense short-term droughts, especially in deforested areas where reduced forest cover lowers soil water retention (Figure 8). At SPI_3, deficits persist through entire seasons, affecting water availability for vegetation and people. At SPI_6 (Figure 8), the cumulative effect of prolonged droughts makes recovery difficult, with strongest impacts in the northwestern and eastern sectors, both of which have high deforestation rates and declining water regimes(Mateus et al., 2025; May et al., 2020).

Conversely, some central DRB areas with higher native vegetation density show weakly positive SPI trends ($\tau > 0.35$), indicating increased moisture or reduced drought frequency (See Supplementary Material, Figures 1 and 2). However, these positive trends are localized and insufficient to compensate for widespread drought impacts in more degraded areas.

Overall, negative SPI_3 and SPI_6 trends suggest that loss of forest cover is undermining key ecosystem services, such as hydrological regulation and carbon sequestration, thus amplifying drought and climate change impacts (A. T. Lima et al., 2021). In the west and south, intensified human pressures and native vegetation loss further exacerbate water deficits and hinder ecosystem recovery.

Dry Season (JJA)

SPI trend analysis for JJA (Figure 8 and 9) reveals that the most significant negative trends ($\tau < -1.5$) are concentrated in the north, where drought frequency and intensity have increased in areas already stressed by deforestation (Figures 1 and 2) . These trends intensify water deficits and reduce ecosystem recovery (Cuartas et al., 2022; Salomão et al., 2020).

At SPI_3 and SPI_6, prolonged deficits become more pronounced, although affecting smaller areas. Reduced water availability limits native species regeneration, favors drought-resistant species, and leads to functional changes that harm biodiversity and ecosystem resilience (Morais et al., 2025). The convergence of negative SPI trends and deforested areas is critical, as forest loss reduces infiltration and aquifer recharge while increasing runoff and drought impacts. Southern and western DRB (See Supplementary Material, Figures 1 and 2), with intense deforestation, exhibit the highest water deficits, likely to worsen with decreased SACZ activity (Lyra & Rigo, 2019).

Conversely, central and northern areas with more forest cover show positive SPI trends and greater water resilience, underlining the importance of native vegetation for hydrological regulation during the dry season (Kulesza & Hościło, 2024; Vicente-Serrano et al., 2013)

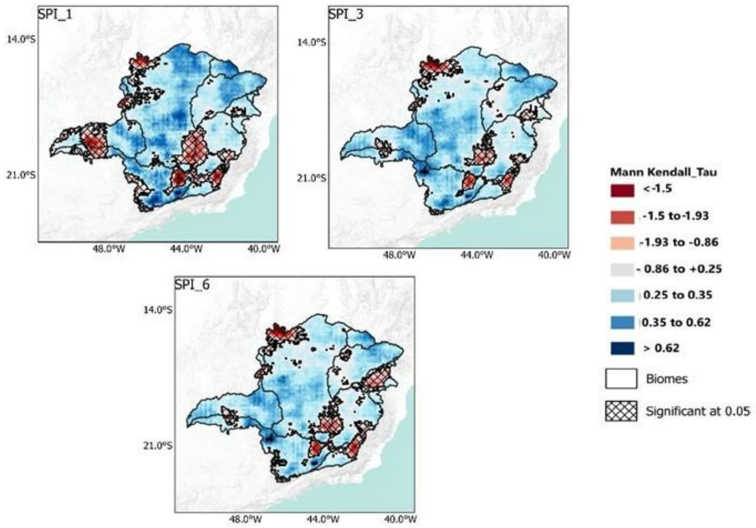

Figure 8. Spatial distribution of Mann-Kendall tau values (2000–2023) for Minas Gerais basins (DJF) using SPI indices at different time scales: SPI_1, SPI_3, and SPI_6. Positive trends (blue) and negative trends (red) highlight areas with significant increases

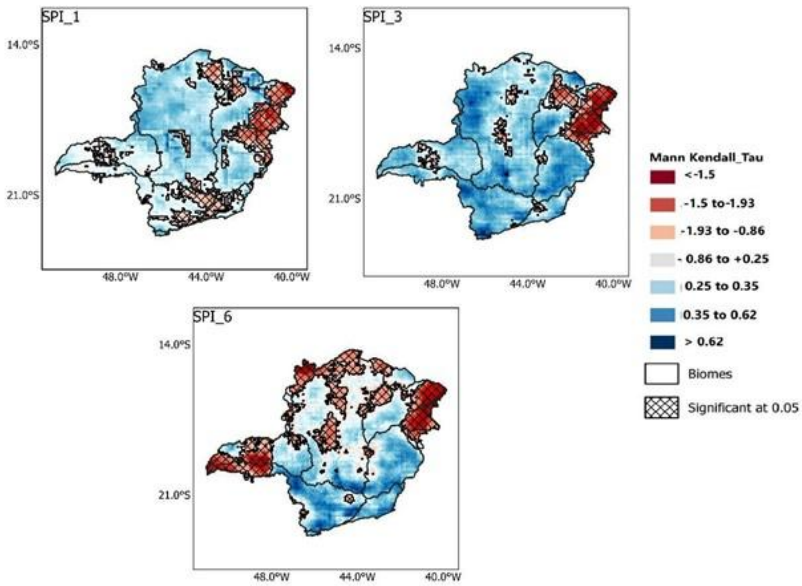

Figure 9. Same as Figure 8, but for dry season (JJA).

Connection Between SPI and EVI

For SPI_1, which assesses short-term droughts (monthly scale), the significant coherence on the 8 to 16-month scale during the periods 2000–2004 and 2014–2016 highlights that vegetation response to drought events is out of phase, with EVI leading (arrows inclined to the left and downward). This suggests that the prior condition of vegetation is a key factor in modulating the impacts of drought, particularly during short periods of water deficit in the basin (Peixoto et al., 2008; Salomão et al., 2020). From 2014 to 2016, marked by the Fundão dam disaster (2015) and a strong El Niño, environmental degradation and changes in water flows amplified the effects of droughts, making vegetation recovery difficult even after subsequent rainfall events(Dutra et al., 2024; Mateus et al., 2025).

On the 2 to 4-month scale, significant coherence observed in 2008, 2014, and 2016 reinforces the sensitivity of vegetation to short-term droughts, although the response is delayed and modulated by factors such as degraded soils and forest fragmentation in the basin (Figure 10). The drought induced by the 2015–2016 El Niño, for example, had immediate effects on vegetation, while the environmental disaster exacerbated water deficit conditions by limiting water infiltration and intensifying surface runoff(J. G. S. Neves et al., 2024). These conditions prevented vegetation from quickly reflecting the benefits of subsequent rainfall.

For SPI_3, significant coherence on the 8–16-month scale (2000–2004) shows that EVI leads drought events, indicating vegetation's dependence on prior cumulative conditions, especially during seasonal droughts (Cui et al., 2025; Zhang et al., 2025). In 2012, 2015, and 2016, coherence on the 2–4-month scale further highlights the impact of moderate droughts on vegetation.

For SPI_6, which captures long-term droughts, the strongest coherence occurs in 2019 and 2022 on the 2–8-month scale, again with EVI leading. However, the signal is weaker than for SPI_1 and SPI_3, suggesting vegetation responds more gradually to prolonged droughts. At larger scales (32–64 months), coherence falls outside the cone of influence, indicating that extremely long-term droughts have a less reliable relationship with vegetation dynamics.

Comparing the indices, SPI_1 reveals the most immediate vegetation response to short-term droughts (2–4 months, EVI leading). SPI_3 shows significant seasonal impacts (8–16 months), while SPI_6 indicates a more diffuse response to prolonged droughts, with weaker coherence.

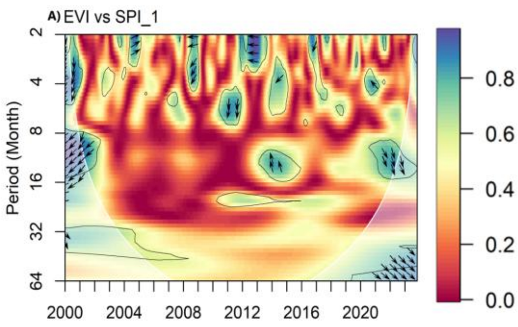

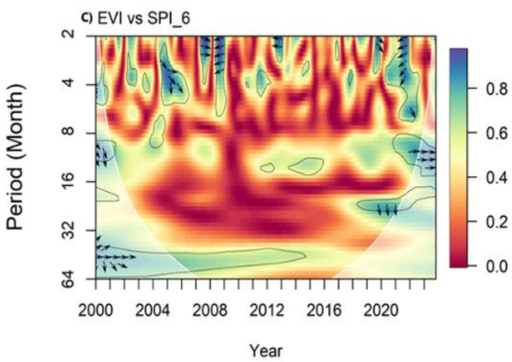

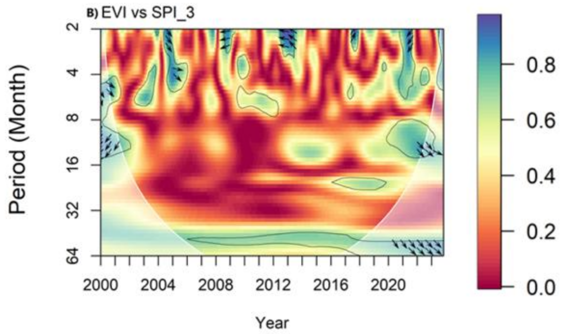

Figure 10 - Wavelet Coherence Analysis between EVI and SPI_1, SPI_3, and SPI_6 Indices for the DRB (2000–2023).

Conclusions

The analysis of interactions between extreme climate events and vegetation in the DRB reveals that vegetation response patterns are shaped by both climate variability and deforestation. The most severe impacts are concentrated in the northern, northwestern, western, southern, and southwestern basin areas, with intense droughts, pronounced precipitation deficits, and high forest loss. Forest fragmentation increases vegetation vulnerability, limiting adaptation and recovery during prolonged water deficits.

Cross-wavelet coherence analysis identified three main temporal scales of vegetation response:

8–16 months: This is the primary window of response, with strong coherence between EVI and precipitation indices (PRCPTOT, RX1day, RX5day), indicating vegetation recovery lags behind extreme precipitation, especially in deforested areas with low soil moisture retention.

2–8 months: Vegetation responds more rapidly to drought, notably SPI_1, SPI_3, and SPI_6, with phase-shifted coherence in degraded areas post-Mariana disaster, highlighting declining resilience after major disturbances.

>34 months: Coherence is weak or absent, suggesting that local factors (soil, fragmentation, land use) outweigh direct climatic controls on vegetation dynamics at these scales.

Extreme precipitation indices (RX1day, RX5day) showed short-term coherence (≤4 months) with vegetation, reflecting rapid response to intense rainfall. In contrast, CDD responses were weaker and slower, indicating cumulative drought impacts. The mismatch between rapid degradation (drought response, 2–4 up to 8 months) and slower recovery (precipitation response, 8–16 months) highlights an imbalance, with degradation outpacing regeneration and increasing vulnerability. Spatial overlap of negative SPI_3 and SPI_6 trends with deforested areas demonstrates that vegetation loss amplifies drought impacts and disrupts hydrological regulation. Conversely, well-preserved forest areas showed localized positive trends, underscoring the stabilizing role of vegetation.

These findings stress the urgency of conservation and restoration to build resilience and mitigate extreme climate impacts. Public policies aimed at sustainable management and recovery of degraded areas are critical for hydrological regulation and reducing basin vulnerability.

Finally, this study underscores the value of a multi-scale approach to understanding vegetation–climate interactions. Further research should explore large-scale drivers, land-use change, and ecological adaptation to improve resource management and inform effective mitigation strategies in the DRB.

Acknowledgments

To the Graduate Program in Analysis and Modeling of Environmental Systems and to the Coordination for the Improvement of Higher Education Personnel (CAPES) for their valuable support.

References

Almeida, F. C. de, Silveira, E. M. de O., Junior, F. W. A., França, L. C. de J., Bueno, I. T., & Terra, B. J. O. (2020). ANÁLISE Multicritério na definição de áreas prioritárias para recuperação florestal na bacia do rio doce, em minas GERAIS. *Nativa*.https://doi.org/10.31413/nativa.v8i1.8130

Alsubih, M., Mallick, J., Alqadhi, S., & Hang, H. T. (2025). Spatiotemporal analysis of drought severity and vegetation health using wavelet coherence: A case study in arid regions of Saudi Arabia. Theoretical and Applied Climatology, 156(3), 159. https://doi.org/10.1007/s00704-025-05390-6

Belhaj, F., Rachid, H., Abdessalam, O., Tariq, A., Abdeldjalil, B., Mohamed, B., Alzahrani, H., Mustafa, H., & El-Askary, H. M. (2025). Predicting precipitation and NDVI utilization of the multi-level linear mixed-effects model and the CA-markov simulation model. *Climate Services*, *38*, 100554. https://doi.org/10.1016/j.cliser.2025.100554

Campos, J. A., da Silva, D. D., Pires, G. F., Amorim, R. S. S., de Menezes Filho, F. C. M., de Melo Ribeiro, C. B., Lorentz, J. F., & Aires, U. R. V. (2024). Modeling Environmental Vulnerability for 2050 Considering Different Scenarios in the Doce River Basin, Brazil. *Water*, *16*(10), 1459. https://www.mdpi.com/2073-4441/16/10/1459#

Carmo, F. F. do, Kamino, L. H. Y., Junior, R. T., Campos, I. C. de, Carmo, F. F. do, Silvino, G., Castro, K. J. da S. X. de, Mauro, M. L., Rodrigues, N. U. A., Miranda, M. P. de S., & Pinto, C. E. F. (2017). Fundão tailings dam failures: The environment tragedy of the largest technological disaster of Brazilian mining in global context. *Perspectives in Ecology and Conservation*, *15*(3), 145–151. https://doi.org/10.1016/j.pecon.2017.06.002

Chervenkov, H., & Slavov, K. (2021). ETCCDI Climate Indices for Assessment of the Recent Climate over Southeast Europe. Em I. Dimov & S. Fidanova (Orgs.), *Advances in High Performance Computing* (p. 398–412). Springer International Publishing. https://doi.org/10.1007/978-3-030-55347-0_34

Cordeiro, J., Gomes, A. R., Santos, C. H. B., Rigobelo, E. C., Baptista, M. B., Moura, P. M., & Scotti, M. R. (2022). Rehabilitation of the Doce River Basin after the Fundão dam collapse: What has been done, what can be done and what should be done? *River Research and Applications*, *38*(2), 194–208. https://doi.org/10.1002/rra.3894

Cuartas, L. A., Cunha, A. P. M. do A., Alves, J. A., Parra, L. M. P., Deusdará-Leal, K., Costa, L. C. O., Molina, R. D., Amore, D., Broedel, E., & Seluchi, M. E. (2022). Recent hydrological droughts in Brazil and their impact on hydropower generation. *Water*, *14*(4), 601. https://doi.org/10.3390/w14040601

Cui, S., Gao, J., Sun, F., Li, G., & Che, Y. (2025). Comparison of vegetation responses to diverse water sources in the Yangtze River Basin: Insights from meteorological, hydrological, and agricultural drought. *Ecological Indicators*, *175*, 113524. https://doi.org/10.1016/j.ecolind.2025.113524

Cunha, A. P. M. A., Zeri, M., Deusdará Leal, K., Costa, L., Cuartas, L. A., Marengo, J. A., Tomasella, J., Vieira, R. M., Barbosa, A. A., Cunningham, C., Cal Garcia, J. V., Broedel, E., Alvalá, R., & Ribeiro-Neto, G. (2019). Extreme Drought Events over

Brazil from 2011 to 2019. *Atmosphere*, *10*(11). https://doi.org/10.3390/atmos10110642

Cupolillo, F., de Abreu, M. L., & Vianello, R. L. (2008). Climatologia da bacia do rio Doce e sua relação com a topografia local. *Revista Geografias*, *4*(2), 45–60.

Copernicus. Global Climate Highlights 2024. Retrieved July 14, 2025, from https://climate.copernicus.eu/global-climate-highlights-2024.

Carvalho, D. R., Ferreira, F. F., Dergam, J. A., Moreira, M. Z., & Pompeu, P. S. (2024). Food web structure of fish communities of Doce River, 5 years after the Fundão dam failure. *Environmental Monitoring and Assessment*, *196*(3), 300. https://doi.org/10.1007/s10661-024-12395-7

Dong, Z., Jia, W., Sarukkalige, R., Fu, G., Meng, Q., & Wang, Q. (2020). Innovative Trend Analysis of Air Temperature and Precipitation in the Jinsha River Basin, China. Water, 12(11), 3293. https://doi.org/10.3390/w1211329.

de Souza, D. C., Crespo, N. M., da Silva, D. V., Harada, L. M., de Godoy, R. M. P., Domingues, L. M., Luiz, R., Bortolozo, C. A., Metodiev, D., de Andrade, M. R. M., Hartley, A. J., de Abreu, R. C., Li, S., Lott, F. C., & Sparrow, S. (2024). Extreme rainfall and landslides as a response to human-induced climate change: A case study at Baixada Santista, Brazil, 2020. *Natural Hazards*, *120*(12), 10835–10860. https://doi.org/10.1007/s11069-024-06621-1

Díaz Baca, M. F., Moreno Lerma, L., Triana Ángel, N., & Burkart, S. (2024). The relationships between land tenure, cattle production, and climate change – A systematic literature review. *Land Use Policy*, *141*, 107169. https://doi.org/10.1016/j.landusepol.2024.107169

Dutra, D. J., Silveira, M. V. F., Mataveli, G., Ferro, P. D., Magalhães, D. da S., de Medeiros, T. P., Anderson, L. O., & Aragão, L. E. O. e C. de. (2024). Challenges for reducing carbon emissions from Land-Use and Land Cover Change in Brazil. *Perspectives in Ecology and Conservation*, *22*(3), 213–218. https://doi.org/10.1016/j.pecon.2024.04.004

El-Nesr, M. N., Abu-Zreig, M. M., & Alazba, A. A. (2010). *Temperature trends and distribution in the Arabian Peninsula.* *6*(2), 191–203.

Ferreira, M. L. (2024). Extreme rain event highlights the lack of governance to face climate change in the Southeastern coast of Brazil. *Geography and Sustainability*, *5*(1), 29–32. https://doi.org/10.1016/j.geosus.2023.11.001

Foley, W. J., McIlwee, A., Lawler, I., Aragones, L., Woolnough, A. P., & Berding, N. (1998). Ecological applications of near infrared reflectance spectroscopy—A tool for rapid, cost-effective prediction of the composition of plant and animal tissues and aspects of animal performance. Oecologia, 116(3), 293–305. https://doi.org/10.1007/s004420050591

Gao, W., Zheng, C., Liu, X., Lu, Y., Chen, Y., Wei, Y., & Ma, Y. (2022). NDVI-based vegetation dynamics and their responses to climate change and human activities from 1982 to 2020: A case study in the Mu Us Sandy Land, China. *Ecological Indicators*, *137*, 108745.

GILBERT, R. (1987). *Statistical methods for environmental pollution monitoring.*

Grinsted, A., Moore, J. C., & Jevrejeva, S. (2004). Application of the cross wavelet transform and wavelet coherence to geophysical time series. Nonlinear Processes in Geophysics, 11(5/6), 561–566. https://doi.org/10.5194/npg-11-561-2004

Guo, J., Yue, Y., Huai, W., Yan, X., Borthwick, A. G. L., Chai, Y., Li, S., Li, Z., Wang, Y., Miao, C., & Yang, Z. (2025). Original vegetation condition and precipitation growth rate bifurcate sediment flux trend on the Qinghai-Tibet Plateau. *Communications Earth & Environment*, *6*(1), 90. https://doi.org/10.1038/s43247-025-02075-w

He, Q., Wang, M., Liu, K., & Wang, B. (2025). High-resolution Standardized Precipitation Evapotranspiration Index (SPEI) reveals trends in drought and vegetation water availability in China. *Geography and Sustainability*, *6*(2), 100228. https://doi.org/10.1016/j.geosus.2024.08.007.

Hoyos, L. E., Cingolani, A. M., Zak, M. R., Vaieretti, M. V., Gorla, D. E., & Cabido, M. R. (2013). Deforestation and precipitation patterns in the arid Chaco forests of central Argentina. Applied Vegetation Science, 16(2), 260–271. https://doi.org/10.1111/j.1654-109X.2012.01218.x

Hu, W., & Si, B. C. (2016). Technical note: Multiple wavelet coherence for untangling scale-specific and localized multivariate relationships in geosciences. Hydrology and Earth System Sciences, 20(8), 3183–3191. https://doi.org/10.5194/hess-20-3183-2016

IPCC. (2022). AR6 Climate Change 2022: Impacts, adaptation and vulnerability. https://www.ipcc.ch/report/sixth-assessment-report-working-group-ii/.

IPCC. (2023). Climate change 2023: Synthesis report. Contribution of Working Groups I, II and III to the Sixth Assessment Report of the Intergovernmental Panel on Climate Change [Core Writing Team, H. Lee, & J. Romero (Eds.)]. https://www.ipcc.ch/report/ar6/syr/

Irannezhad, M., Liu, J., & Chen, D. (2020). Influential Climate Teleconnections for Spatiotemporal Precipitation Variability in the Lancang-Mekong River Basin From 1952 to 2015. Journal of Geophysical Research: Atmospheres, 125(21), e2020JD033331. https://doi.org/10.1029/2020JD033331

Junior, U. J. da S., Junior, J. A. da S., Almeida, D. N. O. de, Santos, E. M. dos, Paiva, A. L. R. de, Santos, S. M. dos, & Oliveira, L. M. M. de. (2024). Variações sazonais intra e interanual da cobertura vegetal (ndvi e savi) na mata ciliar do bioma caatinga associada ao reservatório de serrinha ii, pe, brasil e sua correlação com o spi e o volume hídrico acumulado. Caminhos de Geografia, https://doi.org/10.14393/RCG259970639

Kogan, F., & and Guo, W. (2017). Strong 2015–2016 El Niño and implication to global ecosystems from space data. International Journal of Remote Sensing, 38(1), 161–178. https://doi.org/10.1080/01431161.2016.1259679

Kirby, J. F., & Swain, C. J. (2004). Global and local isostatic coherence from the wavelet transform. Geophysical Research Letters, 31(24). https://doi.org/10.1029/2004GL021569

Kulesza, K., & Hościło, A. (2024). Coherency and time lag analyses between MODIS vegetation indices and climate across forests and grasslands in the European temperate zone. Biogeosciences, 21(10), 2509–2527. https://doi.org/10.5194/bg-21-2509-2024

Lima, A. T., Bastos, F. A., Junior, F. J. T., Neto, R. R., Gomes, H. I., & Barroso, G. F. (2021). Doce River Large-Scale Environmental Catastrophe: Decision and Policy-Making Outcomes. Em A. A. R. Ioris (Org.), Environment and Development: Challenges, Policies and Practices (p. 133–173). Springer International Publishing. https://doi.org/10.1007/978-3-030-55416-3_5

Lima, J. M., & Assis, W. L. (2025). O papel dos veranicos na variabilidade climática: Bacia hidrográfica do Rio Doce-MG/ES e seu entorno. Revista Brasileira de Climatologia, 36, 100–128. https://doi.org/10.55761/abclima.v36i21.19173

Lins, F. A. C., Montenegro, A. A. de A., Farias, C. W. L. de A., da Silva, M. V., de Souza, W. M., Moura, G. B. de A., da Silva, T. G. F., & Montenegro, S. M. G. L. (2024). Soil moisture and hydrological processes dynamics under climate and land use changes in a semiarid experimental basin, Brazil. Ecohydrology & Hydrobiology, 24(3), 681–697. https://doi.org/10.1016/j.ecohyd.2024.02.001

Lyra, A., Tavares, P., Chou, S. C., Sueiro, G., Dereczynski, C., Sondermann, M., Silva, A., Marengo, J., & Giarolla, A. (2018). Climate change projections over three metropolitan regions in Southeast Brazil using the non-hydrostatic Eta regional climate model at 5-km resolution. Theoretical and Applied Climatology, 132(1–2), 663–682. https://doi.org/10.1007/s00704-017-2067-z

Lyra, B. U., & Rigo, D. (2019). Deforestation impact on discharge regime in the Doce River Basin. Ambiente e Agua - An Interdisciplinary Journal of Applied Science, 14(4), 1. https://doi.org/10.4136/ambi-agua.2370

Macêdo, A. K. S., de Oliveira, T. de C. M., Brighenti, L. S., dos Santos, H. B., & Thomé, R. G. (2024). Socio-environmental impacts on the Doce River basin, Brazil: A review from historic pollution to large disaster events.

International Journal of Environmental Science and Technology, 21(2), 2339–2356. https://doi.org/10.1007/s13762-023-05350-5

Marciano, A. G., Assireu, A. T., Azevedo, S. C. de, Silva, B. C. da, Abreu, A. T. de, & Nalini Júnior, H. A. (2024). Dramatic changes in the confluence morphology drived by an extreme hydrologic pulse: Impacts to River Doce restoration. RBRH, 29, e9. https://doi.org/10.1590/2318-0331.292420230139

Marengo, J. A., Jones, R., Alves, L. M., & Valverde, M. C. (2009). Future change of temperature and precipitation extremes in South America as derived from the PRECIS regional climate modeling system. International Journal of Climatology: A Journal of the Royal Meteorological Society, 29(15), 2241–2255. https://doi.org/10.1002/joc.1863

Marengo, J. A., Nobre, C. A., Seluchi, M. E., Cuartas, A., Alves, L. M., Mendiondo, E. M., Obregón, G., & Sampaio, G. (2015). A seca e a crise hídrica de 2014-2015 em São Paulo. Revista Usp, 106, 31–44.

Marion, F. A., Andres, J., Hendges, E. R., & Belon, K. (2024). Influência da temperatura e da precipitação na variação anual de índices de vegetação em área de floresta estacional semidecidual, no sudoeste do paraná, brasil. revista

Mateus, N. P. A., Pujoni, D. G. F., Cunha, M. A., & Ribeiro, S. C. (2025). The impacts of the spatial variation of south atlantic convergence zone on rainfall, flow and water quality in river doce, Brazil. S. C. https://doi.org/10.26848/rbgf.v18.1.p038-060.

May, P., Barbosa, L. C., Brito, M. C., Fernando, L., Maroun, C., Sánchez, L. E., & Kakabadse, Y. (2020). Mainstreaming climate change in the Rio Doce watershed restoration. IUCN, International Union for Conservation of Nature. https://doi.org/10.2305/iucn.ch.2020.06.en

McKee, B. T. (1995). Drought monitoring with multiple time scales. t: https://ci.nii.ac.jp/naid/ 10028178079

McKee, T. B., Doesken, N. J., & Kleist, J. (1993). The relationship of drought frequency and duration to time scales.

Morais, L. F. de, Cavalcante, A. C. R., Leyton, J. M. O., Costa, C. A. G., Silva, R. G. da, Macedo, V. H. M., Maranhão, S. R., & Cândido, M. J. D. (2025). Modeling techniques for simulating total forage biomass in rangelands of the Caatinga Biome, Brazil. Scientia Agricola, 82, e20230300. https://doi.org/10.1590/1678-992X-2023-0300

Ma, S., Zhou, S., Yu, B., & Song, J. (2024). Deforestation-induced runoff changes dominated by forest-climate feedbacks. Science Advances, 10(33), eadp3964. https://doi.org/10.1126/sciadv.adp3964

Natividade, U. A., Garcia, S. R., & Torres, R. R. (2017). Tendência dos Índices de Extremos Climáticos Observados e Projetados no Estado de Minas Gerais. Revista Brasileira de Meteorologia, 32(4), 600–614. https://doi.org/10.1590/0102-7786324008

Neves, D. de S., Silvério, D. V., Rothe-Neves, M., Ferreira, F. F., Iorio, G. S., & Sperber, C. F. (2024). Changes in land use dynamics following the Fundão dam collapse in the Doce River Basin, Brazil. Total Environment Advances, 12, 200112. https://doi.org/10.1016/j.teadva.2024.200112

Neves, J. G. S., Souza, C. S., Figueiredo, J. C. G., Veloso, C. P. de J., Ávila, M. A. de, Oliveira, O. S. de, Azevedo, I. F. P. de, Santos, R. M. dos, Fernandes, G. W., & Nunes, Y. R. F. (2024). Flora and structure of the naturally regenerating riparian vegetation of the Rio Doce River: Basis for environmental restoration actions. Australian Journal of Botany, 72(6). https://doi.org/10.1071/BT23078

Oliveira, B. R. de, Carvalho-Ribeiro ,Sónia Maria, & and Maia-Barbosa, P. M. (2020). A multiscale analysis of land use dynamics in the buffer zone of Rio Doce State Park, Minas Gerais, Brazil. Journal of Environmental Planning and Management, 63(5), 935–957. https://doi.org/10.1080/09640568.2019.1617681

Oliveira, K. S. S., & Quaresma, V. da S. (2017). Temporal variability in the suspended sediment load and streamflow of the Doce River. Journal of South American Earth Sciences, 78, 101–115. https://doi.org/10.1016/j.jsames.2017.06.009

Paiva, A. C. da E., Martins, M., Canamary, E. A., Rodriguez, D. A., & Tomasella, J. (2024). Inter-basin water transfers under changing climate and land use: Assessing water security and hydropower in the Paraíba do

Sul River basin, Brazil. Journal of South American Earth Sciences, 133, 104707. https://doi.org/10.1016/j.jsames.2023.104707

Paula, A., Magnago, L. F. S., & Tagliaferre, C. (2025). Dinâmica do uso e ocupação da terra e seu efeito na temperatura e na precipitação no bioma Caatinga (Floresta Tropical Sazonamente Seca) - Brasil: Land use and occupation dynamics and its effect on temperature and precipitation in the Caatinga biome (Seasonally Dry Tropical Forest) – Brazil. Revista de Geociências do Nordeste, 11(1), Artigo 1. https://doi.org/10.21680/2447-3359.2025v11n1ID36618

Peixoto, A. L., Silva, I. M., José, O., Simonelli, M., de Jesus, R. M., & Rolim, S. G. (2008). Tabuleiro Forests North of the Rio Doce: Their Representation in the Vale do Rio Doce Natural Reserve, Espírito Santo, Brazil.

PIRH. (2010). Plano Integrado de Recursos Hídricos da Bacia Hidrográfica do Rio Doce-PIRH Bacia do Rio Doce-Volume I. Consórcio Ecoplan-Lume.

Ribeiro, M. P., Menezes, G. P., Figueiredo, G. K. D. A., de Mello, K., & Valente, R. A. (2024). Impacts of urban landscape pattern changes on land surface temperature in Southeast Brazil. Remote Sensing Applications: Society and Environment, 33, 101142. https://doi.org/10.1016/j.rsase.2024.101142

Rickard, T., & Ludwig, D. (2024). Dam the river: Ontological exclusion in global and Brazilian Integrated Water Resources Management. Environmental Science & Policy, 156, 103755. https://doi.org/10.1016/j.envsci.2024.103755

Salomão, C. D. S. C., De Souza Paula, L. G., & Elmiro, M. A. T. (2020). Use of multicriteria analysis to define priority areas for reforestation in the Piranga River Basin, MG, Brazil. Sustentabilidade Em Debate, 11(2), 95–120. https://doi.org/10.18472/sustdeb.v11n2.2020.30468

Santana, F. C., Francelino, M. R., Schaefer, C. E. G. R., Veloso, G. V., Fernandes-Filho, E. I., Santana, A. D. J. P., Timo, L. B., & Rosa, A. P. (2021). Water Quality of the Gualaxo do Norte and Carmo Rivers After the Fundão Dam Collapse, Mariana, MG. Water, Air, & Soil Pollution, 232(4), 155. https://doi.org/10.1007/s11270-021-05113-3

Santos, T. C. dos, Teixeira, A. dos S., Moreira, L. C. J., & Toma, R. S. (2024). Effect of indices on desertification risk: Spatial and hierarchical approach using multinomial logistic regression. Revista Ciência Agronômica, 56, e202292588. https://doi.org/10.5935/1806-6690.20250009

Smith, C., Baker, J. C. A., & Spracklen, D. V. (2023). Tropical deforestation causes large reductions in observed precipitation. Nature, 615(7951), 270–275. https://doi.org/10.1038/s41586-022-05690-1

Silva, J. A. da, Bezerra, J. E. F., Gomes, A. C., Barbosa, F. M., & Lacerda, A. V. de. (2024). Phenological Behavior of Cenostigma pyramidale (Tul.) E. Gagnon & G.P.Lewis in an Area of Caatinga in the Semi-Arid Region of Paraíba. Brazilian Archives of Biology and Technology, 67, e24230723. https://doi.org/10.1590/1678-4324-2024230723

Sondermann, M., Chou, S. C., Lyra, A., Latinovic, D., Siqueira, G. C., Junior, W. C., Giornes, E., & Leite, F. P. (2022). Climate change projections and impacts on the eucalyptus plantation around the Doce River basin, in Minas Gerais, Brazil. Climate Services, 28, 100327. https://doi.org/10.1016/j.cliser.2022.100327

Spek, R. van der, & Derumigny, A. (2025). Fast estimation of Kendall’s Tau and conditional Kendall’s Tau matrices under structural assumptions. Dependence Modeling, 13(1), 20250012. https://doi.org/doi:10.1515/demo-2025-0012

Svenning, J.-C., & Sandel, B. (2013). Disequilibrium vegetation dynamics under future climate change. American Journal of Botany, 100(7), 1266–1286. https://doi.org/10.3732/ajb.1200469

Tian, W., Liu, X., Liu, C., & Bai, P. (2018). Investigation and simulations of changes in the relationship of precipitation-runoff in drought years. Journal of Hydrology, 565, 95–105. https://doi.org/10.1016/j.jhydrol.2018.08.015

Torrence, C., & Compo, G. P. (1998). A Practical Guide to Wavelet Analysis. Bulletin of the American Meteorological Society, 79(1), 61–78. https://doi.org/10.1175/1520-0477(1998)079<0061:APGTWA>2.0.CO;2

Vicente-Serrano, S. M., Gouveia, C., Camarero, J. J., Beguería, S., Trigo, R., López-Moreno, J. I., Azorín-Molina, C., Pasho, E., Lorenzo-Lacruz, J., Revuelto, J., Morán-Tejeda, E., & Sanchez-Lorenzo, A. (2013). Response of vegetation to drought time-scales across global land biomes. Proceedings of the National Academy of Sciences, 110(1), 52–57. https://doi.org/10.1073/pnas.1207068110

Wang, Y., Sun, Y., Cao, X., Wang, Y., Zhang, W., & Cheng, X. (2023). A review of regional and Global scale Land Use/Land Cover (LULC) mapping products generated from satellite remote sensing. ISPRS Journal of Photogrammetry and Remote Sensing, 206, 311–334.

Wei, S., Wang, X., Wang, C., & Xie, Q. (2024). El Niño phase transition by deforestation in the Maritime Continent. npj Climate and Atmospheric Science, 7(1), 3. https://doi.org/10.1038/s41612-023-00548-3

Wang, Y., Xue, Z., Ju, A., Yang, Y., Ren, W., & Wu, C. (2025). Spatial distribution patterns and driving factors of ecosystem services and ecological vulnerability in ecologically fragile areas: A case study of the Zhang-Cheng area. Frontiers in Ecology and Evolution, 13. https://doi.org/10.3389/fevo.2025.1570779

Zhang, J., Hao, Y., Hu, B. X., Huo, X., Hao, P., & Liu, Z. (2017). The effects of monsoons and climate teleconnections on the Niangziguan Karst Spring discharge in North China. Climate Dynamics, 48(1), 53–70. https://doi.org/10.1007/s00382-016-3062-2

Zhang, Y., Liu, Y., Chen, L., Sun, J., Sun, Y., Peng, C., Wang, Y., Du, M., & Wu, Y. (2025). Characterizing Drought Patterns and Vegetation Responses in Northeast China: A Multi-Temporal-Scale Analysis Using the SPI and NDVI. Sustainability, 17(12), Artigo 12. https://doi.org/10.3390/su17125288